Lifetime Measurements of Excited States in ^{172}Pt and the Variation of Quadrupole Transition Strength with Angular Momentum

B. Cederwall,[1,*] M. Doncel,[2] Ö. Aktas,[1] A. Ertoprak,[1,3] R. Liotta,[1] C. Qi,[1] T. Grahn,[4] D. M Cullen,[5] B. S. Nara Singh,[5,†] D. Hodge,[5] M. Giles,[5] S. Stolze,[4] H. Badran,[4] T. Braunroth,[6] T. Calverley,[4] D. M. Cox,[4,‡] Y. D. Fang,[7] P. T. Greenlees,[4] J. Hilton,[4] E. Ideguchi,[7] R. Julin,[4] S. Juutinen,[4] M. Kumar Raju,[7] H. Li,[8] H. Liu,[1] S. Matta,[1] V. Modamio,[9] J. Pakarinen,[4] P. Papadakis,[4,§] J. Partanen,[4] C. M. Petrache,[10] P. Rahkila,[4] P. Ruotsalainen,[4] M. Sandzelius,[4] J. Sarén,[4] C. Scholey,[4] J. Sorri,[4,12,‖] P. Subramaniam,[1] M. J. Taylor,[11] J. Uusitalo,[4] and J. J. Valiente-Dobón[12]

[1]*KTH Royal Institute of Technology, 10691 Stockholm, Sweden*
[2]*Department of Physics, Oliver Lodge Laboratory, University of Liverpool, Liverpool L69 7ZE, United Kingdom*
[3]*Department of Physics, Faculty of Science, Istanbul University, Vezneciler/Fatih, 34134 Istanbul, Turkey*
[4]*epartment of Physics, University of Jyvaskyla, P.O. Box 35, FI-40014 Jyväskylä, Finland*
[5]*Schuster Building, School of Physics and Astronomy, The University of Manchester, Manchester M13 9PL, United Kingdom*
[6]*Institut für Kernphysik, Universität zu Köln, 50937 Köln, Germany*
[7]*Research Center for Nuclear Physics, Osaka University, JP-567-0047 Osaka, Japan*
[8]*Grand Accélérateur National dâ Ions Lourds (GANIL), CEA/DSMâ CNRS/IN2P3, F-14076 Caen Cedex 5, France*
[9]*Department of Physics, University of Oslo, NO-0316 Oslo, Norway*
[10]*Centre de Sciences Nucléaires et Sciences de la Matière, CNRS/IN2P3, Université Paris-Saclay, 91405 Orsay, France*
[11]*Division of Cancer Sciences, School of Medical Sciences, The University of Manchester, Manchester, M13 9PL, United Kingdom*
[12]*Istituto Nazionale di Fisica Nucleare, Laboratori Nazionali di Legnaro, I-35020 Legnaro, Italy*

Lifetimes of the first excited 2^+ and 4^+ states in the extremely neutron-deficient nuclide ^{172}Pt have been measured for the first time using the recoil-distance Doppler shift and recoil-decay tagging techniques. An unusually low value of the ratio $B(E2{:}4_1^+ \to 2_1^+)/B(E2{:}2_1^+ \to 0_{\rm gs}^+) = 0.55(19)$ was found, similar to a handful of other such anomalous cases observed in the entire Segré chart. The observation adds to a cluster of a few extremely neutron-deficient nuclides of the heavy transition metals with neutron numbers $N \approx 90$–94 featuring the effect. No theoretical model calculations reported to date have been able to explain the anomalously low $B(E2{:}4_1^+ \to 2_1^+)/B(E2{:}2_1^+ \to 0_{\rm gs}^+)$ ratios observed in these cases. Such low values cannot, e.g., be explained within the framework of the geometrical collective model or by algebraic approaches within the interacting boson model framework. It is proposed that the group of $B(E2{:}4_1^+ \to 2_1^+)/B(E2{:}2_1^+ \to 0_{\rm gs}^+)$ ratios in the extremely neutron-deficient even-even W, Os, and Pt nuclei around neutron numbers $N \approx 90$–94 reveal a quantum phase transition from a seniority-conserving structure to a collective regime as a function of neutron number. Although a system governed by seniority symmetry is the only theoretical framework for which such an effect may naturally occur, the phenomenon is highly unexpected for these nuclei that are not situated near closed shells.

Introduction.—The excitation energies and lifetimes of the first excited 2^+ and 4^+ states in atomic nuclei with even numbers of neutrons and protons are fundamental observables in nuclear structure physics. These quantities constitute key benchmarks for testing and differentiating between essentially all available nuclear models, from the "single-particle" to the collective regime. In particular, the reduced electric quadrupole transition probability, $B(E2)$, directly probes the wave functions of the lowest-lying excited states and the ground state.

The emergence of collective behavior in atomic nuclei outside closed-shell configurations represents one of the most important, still least understood, paradigms in the description of finite many-body quantum systems [1]. Nuclei, with their coexisting neutron and proton Fermi liquids, add complexity and uniqueness to this problem.

In general, several nucleons or more away from the "magic" neutron and proton numbers (which reflect major gaps in the energy level spectrum), an emergence of collectivity is observed. This signals that the wave function spreads to multiple coherent particle-hole components, opening the vibrational or rotational degrees of freedom, and is normally associated with a lowering of the first excited 2_1^+ state energy accompanied by an increase in the $2_1^+ \rightarrow 0_{gs}^+$ reduced transition strength. A gradual evolution of electric quadrupole strength, i.e., $B(E2:2_1^+ \rightarrow 0_{gs}^+)$ values, is then expected along an isotopic chain: from spherical systems near closed shells where the $B(E2)$ strength is at a minimum and governed by the individual single-particle degrees of freedom, via quadrupole surface vibrations around spherical symmetry, to the gradual development of deformation towards well-developed axially symmetric shapes with their associated rotational excitations and maximal $B(E2)$ values when the Fermi level is situated in the middle between major shell closures.

The $B(E2)$ values usually increase with spin for low-lying states within a collective (rotational or vibrational) band structure [2]. As a consequence, the $B(E2:4_1^+ \rightarrow 2_1^+)/B(E2:2_1^+ \rightarrow 0_{gs}^+)$ ratio ($B_{4/2}$) is strictly larger than unity for collective excitations. For an ideal rotor, a value of $B_{4/2} = 10/7 = 1.43$ is expected (known as the Alaga rule), whereas for a harmonic vibrator, $B_{4/2} = 2$, reflecting the ratio between the number of phonons in the initial state for each transition. Notably, in our current understanding of nuclear structure, the only possible exceptions are structures exhibiting seniority symmetry near magic neutron and/or proton numbers or shape-coexisting structures (although in the latter scenario, there are no known cases with $B_{4/2} < 1$).

We here report on the first measurement of lifetimes of excited states in the extremely neutron-deficient nucleus ^{172}Pt, 18 neutrons removed from the nearest stable platinum isotope ^{190}Pt and with its 78 protons and 94 neutrons well separated from the closest magic neutron and proton numbers at $N = Z = 82$.

Experimental details.—Excited states in ^{172}Pt were populated in fusion-evaporation reactions induced by a ^{83}Kr beam produced by the K-130 cyclotron at the University of Jyväskylä (JYFL), Finland. The ^{83}Kr ions were accelerated to a bombarding energy of 383 MeV and let to impinge on a self-supporting, isotopically enriched ^{92}Mo metallic target foil with an areal density of 0.52 mg/cm^2. The ^{172}Pt fusion-evaporation residues were produced in the (^{83}Kr, 3n) reaction channel. The experimental setup consisted of the JUROGAM II high-purity germanium detector array [3,4] coupled to the RITU gas-filled electromagnetic recoil separator [5] and the differential plunger for unbound nuclear states (DPUNS) [6]. The DPUNS device was equipped with a 1 mg/cm^2 thick natural Mg degrader foil, which decreased the average velocity of the recoiling fusion residues by approximately 15%. The degrader was placed downstream the thin ^{92}Mo target foil, which could be moved to different positions relative to the degrader. The RITU separator was used to discriminate the beam particles from the fusion residues by measuring the energy loss in a multiwire proportional counter (MWPC) and the time of flight of recoils measured between the MWPC and the two double-sided silicon strip detectors (DSSSD) of the focal plane detector system GREAT [7], in which the fusion residues were implanted. The prompt γ rays emitted in delayed coincidence with the recoiling fusion products were measured with JUROGAM II, which consisted of 15 phase-I-type and 24 clover detectors from the former EUROBALL detector array [8] arranged in four rings, resulting in a photopeak efficiency of ~6% at 1.3 MeV γ-ray energy. However, only the detectors located at angles 134° and 158° with respect to the beam direction, where the Doppler shift is large enough, were employed in the present analysis. Ten different target-to-degrader distances, ranging from 10 to 2000 μm, were used for the lifetime analysis.

Method and analysis.—The low production cross section for the nucleus ^{172}Pt, approximately 10^{-5} of the total fusion cross section, required recoil-decay tagging [9–11] to select the rare γ-ray events from the vast background of γ rays from the multitude of different fusion-evaporation residues closer to the β-stability line. The rare fusion-evaporation reactions leading to ^{172}Pt were identified using the characteristic α-decay properties of the recoiling nuclei [$E_\alpha = 6.314(4)$ MeV, $t_{1/2} = 96(3)$ ms [12]]. The short half-life of ^{172}Pt and its large α-decay branching ratio of approximately 94% [13] enabled clean and efficient selection of the ^{172}Pt ions [12]. The lifetime analysis could therefore be performed using single γ-ray energy spectra recorded in delayed coincidence with 6.314(4) MeV α particles detected in the DSSSD detectors at the focal plane of the RITU recoil separator for each target-to-degrader distance. Typical γ-ray energy spectra and normalized decay intensities used in the lifetime determination for the first excited 2^+ and 4^+ states in ^{172}Pt are shown in Figs. 1 and 2, respectively.

The lifetime analysis was performed following the principles of the recoil-distance Doppler shift technique [14,15] and the differential decay curve method [16]. The lifetimes of the first excited 2^+ and 4^+ states in ^{172}Pt have been extracted (see Fig. 2) using the following equation:

$$\tau_i(x) = -\frac{Q_{ij}(x) - \sum_h \alpha_h Q_{hi}(x)}{\frac{d}{dx}\{Q_{ij}(x)\}} \frac{1}{\langle v \rangle}, \qquad (1)$$

where i indicates the state of interest, while h and j denote states above and below it in a γ-ray cascade, respectively.

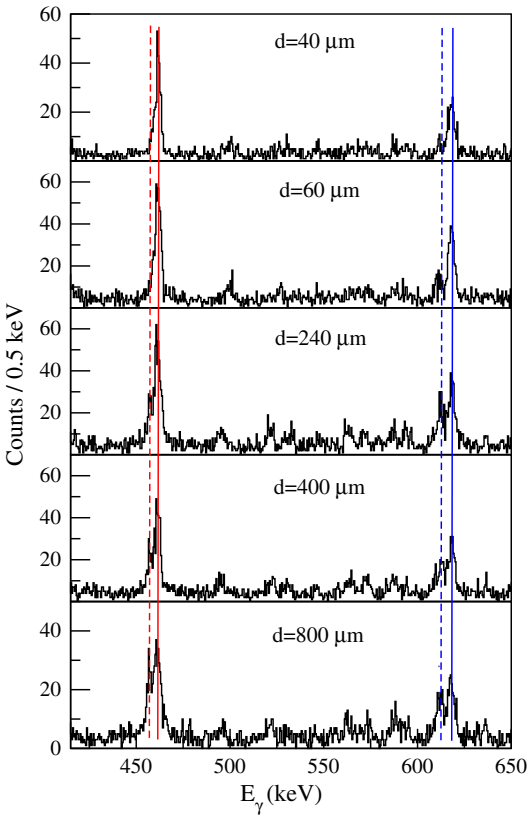

FIG. 1. Alpha-decay-tagged γ-ray energy spectra used for the lifetime determination in ^{172}Pt for five different target-to-degrader distances. The centroids for the $2_1^+ \rightarrow 0_{gs}^+$ 458 keV γ-ray transition when emitted before (after) the degrader foil are indicated by vertical red dashed (solid) lines, while the centroids for the $4_1^+ \rightarrow 2_1^+$ 612 keV γ-ray transition when emitted before (after) the degrader foil are indicated by vertical blue dashed (solid) lines.

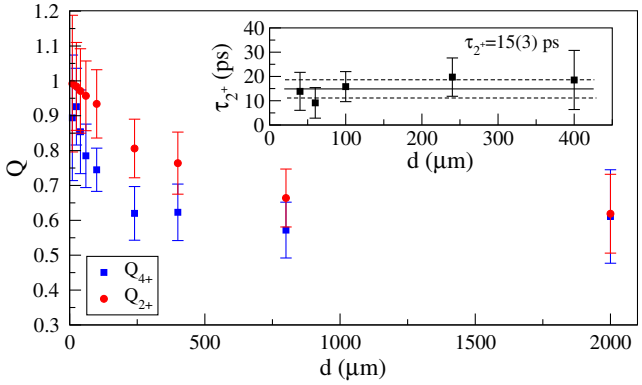

FIG. 2. Normalized γ-ray intensity, $Q = I_{after}/(I_{after} + I_{before})$, where the subscripts "after" and "before" refer to γ rays emitted after and before the degrader foil, respectively) as a function of target-to-degrader distance for the $2_1^+ \rightarrow 0_{gs}^+$ (red symbols) and $4_1^+ \rightarrow 2_1^+$ (blue symbols) transitions in ^{172}Pt. (Inset) Lifetime of the 2_1^+ state in ^{172}Pt evaluated for five target-to-degrader distances in the region of sensitivity along with the weighted mean of 15 ps (solid line) and its uncertainty ± 3 ps (dashed lines).

The quantities $Q_{ij}(x)$ and $Q_{hi}(x)$ are the normalized intensities of the degraded components of depopulating and feeding transitions, while $(d/dx)\{Q_{ij}(x)\}$ is the slope of the intensity as a function of distance x (deduced using the code APATHIE [17]). The mean recoil velocity directly after the target was determined to be $\langle v \rangle = 0.0445(5)c$. The factors α_h are given by

$$\alpha_h(x) = -\frac{Q_{ij}^s + Q_{ij}^d}{Q_{hi}^s + Q_{hi}^d}, \qquad (2)$$

where Q^s and Q^d correspond to normalized intensities of the fully Doppler-shifted and degraded components of the photopeak, respectively, and account for the differences in intensities between feeding and depopulating transitions. The intensities of relevant γ-ray transitions were deduced using the RADWARE data analysis package [18], taking into account detector efficiency, and found to be in agreement with previous work [12,19]. Lifetime values of $\tau = 15 \pm 3$ ps and $\tau = 6.2 \pm 1.7$ ps have been deduced for the 2_1^+ and 4_1^+ states in ^{172}Pt, respectively. The results are summarized in Table I. The resulting value of $B_{4/2} = 0.55(19)$ is unusually low and its possible interpretation is discussed below.

Discussion.—Platinum and neighboring elements in the periodic table have exceptionally long isotopic chains between closed neutron shells for which the excitation energies of the lowest excited states are known, providing a valuable testing ground for studies of collective behavior. The excitation energy systematics of the first excited 2^+ and 4^+ states in the platinum isotopes with even neutron numbers N appear to follow the expected evolution of collectivity as a function the Fermi level within the major $N = 82$–126 shell: from near-spherical structures exhibiting collective vibrations in the most neutron-deficient species with known excited states ($N = 90$–92 [20]) followed by a transition to a weakly deformed collective rotational structure in ^{172}Pt [12] ($N = 94$), via soft triaxial rotors $N = 96$–98 [21,22], to well-deformed prolate shapes ($N \geq 100$) towards the neutron midshell at $N = 104$ [21,23,24] [see Fig. 3(a)]. Beyond the neutron midshell, the excitation energy systematics indicate that collectivity again decreases towards the next major shell

TABLE I. Energies of the $2_1^+ \rightarrow 0_{gs}^+$ and $4_1^+ \rightarrow 2_1^+$ transitions (E_γ), deduced lifetime values (τ) for the 2_1^+ and 4_1^+ states, and corresponding reduced transition probabilities $[B(E2\downarrow)_{exp}]$ in Weisskopf units (W.u.).

Transition	E_γ (keV)	τ (ps)	$B(E2\downarrow)_{exp}$ (W.u.)
$2_1^+ \rightarrow 0_{gs}^+$	458	15(3)	49(11)
$4_1^+ \rightarrow 2_1^+$	612	6.2(17)	27(7)

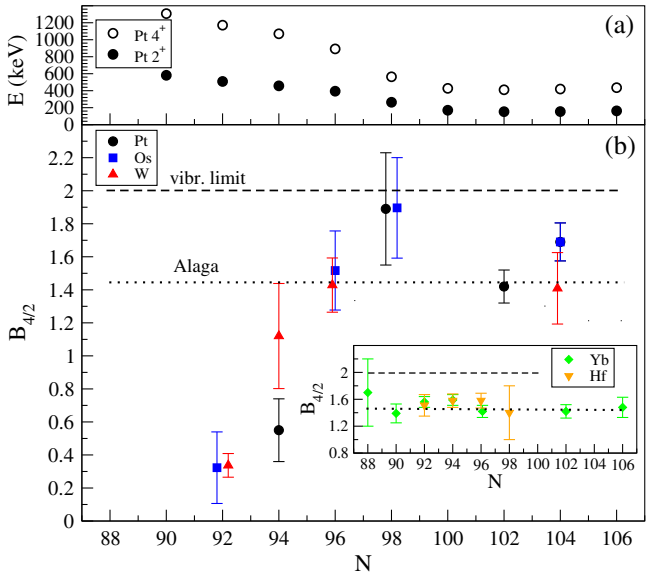

FIG. 3. (a) Evolution of 2_1^+ and 4_1^+ energies for Pt isotopes as a function of neutron number N. (b) Experimental $B(E2:4_1^+ \to 2_1^+)/B(E2:2_1^+ \to 0_{gs}^+)$ ratios (when available) for the even-even tungsten, osmium, and platinum isotopes with neutron numbers $88 \leq N \leq 106$. (Inset) The corresponding ratios (when available) for the even-even ytterbium and hafnium isotopes with neutron numbers $88 \leq N \leq 106$. The experimental data are from this Letter and Refs. [25–28]. Some of the data points have been shifted slightly to the left or right for better legibility.

closure at $N = 126$, due to the gradually reduced valence space.

Furthermore, the Pt nuclei with $N \geq 96$ and close to midshell are found to lie close to a region of shape coexistence [21–24,29]. The appearance of shape coexistence in atomic nuclei, another phenomenon that is unexpected from first principles, remains one of the most intensely studied subjects in nuclear structure physics for several decades. Among a multitude of studies of shape coexistence, the triple shape coexistence in ^{186}Pb reported by Andreyev *et al.* [30] is one of the highlights. Such phenomena are now known to occur in various regions of the Segré chart [29,31–33]. Shape polarization effects in nuclei are generally associated with two-particle-two-hole ($2p$-$2h$) excitations and/or with the occupation of specific shape driving orbits such as the high-j unique parity (intruder) levels [33]. The polarizing effect of such configurations may lead to "softness" of the nuclear shape with respect to deformation, to low-lying quadrupole phonon excitations, and to shape-coexistence phenomena. An alternative description can be provided by interacting boson model (IBM) calculations. IBM-1 calculations within the extended consistent Q formalism describe reasonably the level energies and the $B(E2)$ transition strengths of several even-even Pt isotopes [34]. If the ground state and the 2_1^+ state belong to a different coexisting collective structure than the 4_1^+ state, a ratio $B_{4/2} < 1$ is, in principle, possible, although it has never been observed for yrast transitions. For instance, in the mercury isotopes that are also known to exhibit shape coexistence, the higher lying transitions are always more collective than the $2_1^+ \to 0_{gs}^+$ transition [35]. Extensive theoretical model calculations within the beyond-mean-field and IBM frameworks of the structure of the platinum isotopes provide similar results [36–38].

The only standard theoretical model scenario in which $B_{4/2} < 1$ naturally may occur is when seniority (defined as the number of unpaired nucleons) is a good quantum number, i.e., in a system dominated by strong pairing correlations. Well-known cases are singly closed-shell, "semimagic" nuclei, which are well described by the seniority pair-coupling scheme when the structure is dominated by a single-j subshell [39–41]. Seniority symmetry leads to opposite trends in the reduced transition probabilities for seniority-conserving and nonconserving transitions as a function of shell filling. In a configuration with n particles in a j subshell, the strength of the seniority nonconserving $2_1^+ \to 0_{gs}^+$ transition $[B(E2:2_1^+ \to 0_{gs}^+)]$ increases, while the strength of the seniority-conserving $4_1^+ \to 2_1^+$ transition $[B(E2:4_1^+ \to 2_1^+)]$ decreases with n to a maximum and minimum, respectively, at midshell [41–43]. Thereafter, $B(E2:2_1^+ \to 0_{gs}^+)$ and $B(E2:4_1^+ \to 2_1^+)$ will decrease and increase, respectively, until the subshell is filled. Hence, in this scenario, $B_{4/2} < 1$ may occur around midshell and thereafter increase rapidly as a function of n. Interestingly, such textbook patterns of seniority symmetry are quite rare, although a handful of cases with $B_{4/2} < 1$ in magic and near magic nuclei in the lead, tin, and some other regions have been observed [25,26,44–48]. Figure 3(b) shows the experimental $B_{4/2}$ ratios reported to date (including the $B_{4/2}$ value derived for ^{172}Pt in the present Letter) for the even-even tungsten, osmium, and platinum isotopes with neutron numbers $88 \leq N \leq 106$. A pattern that is consistent with the expectations in the presence of seniority symmetry appears for the most neutron-deficient nuclei with $N \leq 94$. For larger neutron numbers, the $B_{4/2}$ ratios increase and enter the collective regime between the vibrational and rotational limits. As a comparison, we show the corresponding experimental $B_{4/2}$ values for the ytterbium and hafnium isotones (where known) (see inset of Fig. 3). These nuclei exhibit $B_{4/2}$ ratios around the rotational limit of the collective model (Alaga rule). The mercury isotones (not shown) consistently have significantly higher $B_{4/2}$ ratios with values around 2–5 [28]. Hence, while the $B_{4/2}$ ratios for the corresponding Yb and Hf isotones clearly indicate stable, deformed rotational structures, the values shown in Fig. 3 for the W, Os, and Pt isotopes reveal clear evidence for seniority symmetry for $N \leq 94$, followed by a transition to the collective regime for larger neutron numbers. The mercury isotopes (not shown), on the other hand, reveal patterns that are in agreement with what is expected

from shape coexistence and a transition to a more collective structure with increasing angular momentum [35].

This unusual situation indicates that the W, Os, and Pt nuclides with $N \leq 94$ might obey seniority symmetry, despite the fact that they are four or more protons and eight or more neutrons removed from the nearest closed shells at Z or $N = 82$. It should be noted that seniority symmetry was previously mentioned and excluded as a plausible scenario in the cases of ^{168}Os [25] and ^{166}W [26] for this particular reason. However, the nuclei for which $B_{4/2} < 1$ in Fig. 3 are considered to have near-spherical shapes, and we also note that the position of the neutron Fermi level within the *mixed* ($\nu h_{9/2} f_{7/2}$) subshell is perfectly placed at, and just above, midshell in order to explain the observed effect. Unfortunately, due to the large model spaces involved, nuclei such as ^{172}Pt are typically well beyond the scope of current state-of-the-art shell model calculations employing modern high-performance computing. The experimental findings therefore remain a major challenge for nuclear theory. Nevertheless, we have attempted large-scale shell model calculations for Pt, Os, and W isotopes between $N = 82$ and 94 by considering either ^{132}Sn or ^{146}Gd as inert cores. All neutron levels between $N = 82$ and 126 were included, but otherwise, certain truncations in the model space were necessary. The cross-shell neutron-proton interactions were evaluated from the charge-dependent Bonn nucleon-nucleon potential with slight modifications to better reproduce the properties of $N = 84$ isotones [49]. The calculations reproduce reasonably well the excitation energies of the lowest-lying excited states as well as the $B(E2{:}2_1^+ \rightarrow 0_{\mathrm{gs}}^+)$ values for ^{172}Pt and neighboring nuclei. They indicate that the neutron $f_{7/2}$ and $h_{9/2}$ subshell are indeed strongly mixed and nearly degenerate as a result of the attractive neutron-proton $\nu h_{9/2} - \pi h_{11/2}$ monopole interaction. However, reproducing the small $B_{4/2}$ value observed for ^{172}Pt requires that the neutron-proton quadrupole-quadrupole interaction strength is significantly weaker than for the standard nucleon-nucleon interaction used in other mass regions (see, e.g., [50]).

We have surveyed the $B_{4/2}$ systematics known to date [28] in the entire region of the Segré chart, from the tin isotopes to lead. Apart from the semimagic nuclides $\{^{112,114,120,122,124}\mathrm{Sn}\}$ ($Z = 50$), $\{^{134}\mathrm{Te}, ^{136}\mathrm{Xe}, ^{138}\mathrm{Ba}, ^{140}\mathrm{Ce}, ^{142}\mathrm{Nd}\}$ ($N = 82$), and ^{204}Pb ($Z = 82$), there are presently only a few isolated cases with known $B_{4/2} < 1$: ^{98}Ru, ^{114}Te [48], ^{134}Te, ^{134,136}Ce, ^{132,144}Nd, ^{134}Xe, ^{152}Dy, and ^{198}Hg. Hence, the pattern of $B_{4/2}$ values as a function of neutron number N shown in Fig. 3 appears to be rather unique. This pattern indicates a phase transition, or a combination of phase transitions, appearing in the W, Os, and Pt isotopic chains for neutron numbers $N = 92$–96.

The low $B_{4/2}$ values ($B_{4/2} \ll 1$) observed for $N = 92$ indicate the presence of seniority symmetry in a spherical nucleus around midshell as discussed above. The subsequent rise in $B_{4/2}$ as a function of increasing N is in line with the predicted behavior for such a system as the shell filling increases. Subsequently, around $N = 96$, the data are consistent with a transition to the collective regime. Finally, a collective phase transition from the spherical to a deformed phase is indicated by the variation in $B_{4/2}$ values between $N = 98$ and $N = 104$. A nuclear transition from a spherical to a deformed phase was recognized a long time ago [51]. A similar phase transition was found in an IBM study [52] when going from an U(5) to an O(6) symmetry, i.e., from a spherical-vibrator to a deformed-rotor phase.

Summary.—The lifetimes of the first excited 2^+ and 4^+ states in the extremely neutron-deficient nucleus ^{172}Pt have been measured using the recoil-distance Doppler shift technique. An unusually low $B_{4/2}$ value of 0.55(19) is observed. The measurement complements and highlights a cluster of nuclides in the nuclear chart where the ratio of electric quadrupole strength $B_{4/2}$ shows an unexpected systematic behavior, namely, $B_{4/2} < 1$, while other such occurrences in the nuclear landscape are either isolated or in the vicinity of particular regions, i.e., close to magic numbers. It might reveal a pattern indicating a transition from a seniority-conserving structure to a collective regime as a function of neutron number. Although a system governed by seniority symmetry is a possible theoretical framework for which such an effect may naturally occur, the phenomenon is highly unexpected for these nuclei that are not situated near closed shells. This observation and its lack of reproducibility by standard nuclear models underscore the complexity of the atomic nucleus as a many-body quantum system and its proton-neutron duality.

This work was supported by the Swedish Research Council under Grant No. 621-2014-5558, the United Kingdom Science and Technology Facilities Council (STFC), the EU Seventh Framework Programme, Integrating Activities Transnational Access, Project No. 262010 ENSAR, and the Academy of Finland under the Finnish Centre of Excellence Programme (Nuclear and Accelerator Based Physics Programme at JYFL). E. I., Y. D. F., and M. K. R. acknowledge support from the International Joint Research Promotion Program of Osaka University. The authors acknowledge the support of the GAMMAPOOL for the JUROGAM detectors.

[*]Corresponding author.
cederwall@nuclear.kth.se
[†]Present address: School of Engineering and Computing, University of the West of Scotland, Paisley, PA1 2BE, United Kingdom.
[‡]Present address: Department of Physics, Lund University, 221 00 Lund, Sweden.
[§]Present address: Department of Physics, Oliver Lodge Laboratory, University of Liverpool, Liverpool L69 7ZE, United Kingdom.

[‖]Present address: Sodankylä Geophysical Observatory, FI-99600 Sodankylä, Finland.

[1] J. L. Wood, Nuclear Collectivity—Its Emergent Nature Viewed from Phenomenology and Spectroscopy, in *Emergent Phenomena in Atomic Nuclei from Large-Scale Modeling* (World Scientific, Singapore, 2017).
[2] A. Bohr and B. R. Mottelson, *Nuclear Structure* (World Scientific, Singapore, 1998), Vol. II, p. 45.
[3] F. Beck *et al.*, Prog. Part. Nucl. Phys. **28**, 443 (1992).
[4] C. Beausang and J. Simpson, J. Phys. G **22**, 527 (1996).
[5] M. Leino *et al.*, Nucl. Instrum. Methods Phys. Res., Sect. B **99**, 653 (1995).
[6] M. J. Taylor *et al.*, Nucl. Instrum. Methods Phys. Res., Sect. A **707**, 143 (2013).
[7] R. D. Page *et al.*, Nucl. Instrum. Methods Phys. Res., Sect. B **204**, 634 (2003).
[8] J. Simpson, Z. Phys. A **358**, 139 (1997).
[9] K. H. Schmidt, R. S. Simon, J.-G. Keller, F.P. Hessberger, G. Münzenberg, B. Quint, H.-G. Clerc, W. Schwab, U. Gollerthan, and C.-C. Sahm, Phys. Lett. **168B**, 39 (1986).
[10] R. S. Simon, K.-H. Schmidt, F. P. Heßberger, S. Hlavac, M. Honusek, G. Münzenberg, H.-G. Clerc, U. Gollerthan, and W. Schwab, Z. Phys. A **325**, 197 (1986).
[11] E. S. Paul *et al.*, Phys. Rev. C **51**, 78 (1995).
[12] B. Cederwall *et al.*, Phys. Lett. B **443**, 69 (1998).
[13] B. Singh, Nucl. Data Sheets **75**, 199 (1995).
[14] T. K. Alexander and J. S. Foster, Adv. Nucl. Phys. **10**, 197 (1978).
[15] A. Dewald, O. Möller, and P. Petkov, Prog. Part. Nucl. Phys. **67**, 786 (2012).
[16] A. Dewald, S. Harissopulos, and P. Brentano, Z. Phys. A **334**, 163 (1989).
[17] F. Seiffert, Program APATHIE, Institut für Kernphysik, Universitat zu Köln (1989).
[18] D. C. Radford *et al.*, Nucl. Instrum. Methods Phys. Res., Sect. A **361**, 297 (1995).
[19] D. T. Joss *et al.*, Phys. Rev. C **74**, 014302 (2006).
[20] S. L. King *et al.*, Phys. Lett. B **443**, 82 (1998).
[21] G. D. Dracoulis, B. Fabricius, A. E. Stuchbery, A. O. Macchiavelli, W. Korten, F. Azaiez, E. Rubel, M. A. Deleplanque, R. M. Diamond, and F. S. Stephens, Phys. Rev. C **44**, R1246 (1991).
[22] B. Cederwall *et al.*, Z. Phys. A **337**, 283 (1990).
[23] G. D. Dracoulis, A. E. Stuchbery, A. P. Byrne, A. R. Poletti, S. J. Poletti, J. Gerl, and R. A. Bark, J. Phys. G **12**, L97 (1986).
[24] F. Le Blanc *et al.*, Phys. Rev. C **60**, 054310 (1999).
[25] T. Grahn *et al.*, Phys. Rev. C **94**, 044327 (2016).
[26] B. Saygi *et al.*, Phys. Rev. C **96**, 021301(R) (2017).
[27] C. Müller-Gatermann *et al.*, Phys. Rev. C **97**, 024336 (2018).
[28] https://www.nndc.bnl.gov/.
[29] J. L. Wood, K. Heyde, W. Nazarewicz, M. Huyse, and P. van Duppen, Phys. Rep. **215**, 101 (1992).
[30] A. Andreyev, Nature (London) **405**, 430 (2000).
[31] K. Heyde *et al.*, Phys. Rep. **102**, 291 (1983).
[32] K. Heyde and J. L. Wood, Rev. Mod. Phys. **83**, 1467 (2011).
[33] K. Heyde and J. L. Wood, J. Phys. G **43**, 020402 (2016).
[34] E. A. McCutchan, R. F. Casten, and N. V. Zamfir, Phys. Rev. C **71**, 061301R (2005).
[35] N. Bree *et al.*, Phys. Rev. Lett. **112**, 162701 (2014).
[36] R. Rodríguez-Guzmán, P. Sarriguren, L. M. Robledo, and J. E. García-Ramos, Phys. Rev. C **81**, 024310 (2010).
[37] K. Nomura, T. Otsuka, R. Rodríguez-Guzmán, L. M. Robledo, and P. Sarriguren, Phys. Rev. C **83**, 014309 (2011).
[38] J. E. García-Ramos, K. Heyde, L. M. Robledo, and R. Rodríguez-Guzmán, Phys. Rev. C **89**, 034313 (2014).
[39] I. Talmi, *Simple Models of Complex Nuclei* (Harwood Academic Press, Switzerland, 1993).
[40] D. J. Rowe and G. Rosensteel, Phys. Rev. Lett. **87**, 172501 (2001).
[41] R. F. Casten, *Nuclear Structure from a Simple Perspective* (Oxford University Press, New York, 2000).
[42] A. de Shalit and I. Talmi, *Nuclear Shell Theory* (Academic Press, New York, 1963).
[43] J. J. Ressler *et al.*, Phys. Rev. C **69**, 034317 (2004).
[44] R. B. Cakirli, R. F. Casten, J. Jolie, and N. Warr, Phys. Rev. C **70**, 047302 (2004).
[45] D. Hertz-Kintish, L. Zamick, and S. J. Q. Robinson, Phys. Rev. C **90**, 034307 (2014).
[46] C. Louchart *et al.*, Phys. Rev. C **87**, 054302 (2013).
[47] G. de Angelis *et al.*, Phys. Lett. B **535**, 93 (2002).
[48] O. Möller, N. Warr, J. Jolie, A. Dewald, A. Fitzler, A. Linnemann, K. O. Zell, P. E. Garrett, and S. W. Yates, Phys. Rev. C **71**, 064324 (2005).
[49] R. Machleidt, Phys. Rev. C **63**, 024001 (2001).
[50] M. Hjorth-Jensen, T. T. S. Kuo, and E. Osnes, Phys. Rep. **261**, 125 (1995).
[51] D. J. Thouless, Nucl. Phys. **A22**, 78 (1961).
[52] D. J. Rowe, Nucl. Phys. **A745**, 47 (2004).

Correction: The name of the ninth author had been missing in the original publication and has been inserted.